UC Irvine
UC Irvine Previously Published Works

Title

Spectral analysis of spatial sampling by photoreceptors: Topological disorder prevents aliasing

Permalink

https://escholarship.org/uc/item/6cw0h7jv

Journal

Vision Research, 22(9)

ISSN

0042-6989

Author

Yellott, John I

Publication Date

1982

DOI

10.1016/0042-6989(82)90086-4

Peer reviewed

SPECTRAL ANALYSIS OF SPATIAL SAMPLING BY PHOTORECEPTORS: TOPOLOGICAL DISORDER PREVENTS ALIASING

John I. Yellott Jr

Cognitive Science Group, School of Social Sciences, University of California, Irvine, CA 92717, U.S.A.

Abstract—To determine whether the spatial disorder of human photoreceptors is sufficient to prevent aliasing distortion, optical transform techniques were used to compute the power spectrum of a $12' \times 13'$ array of foveal cones treated as sampling points and also the post-sampling spectra of gratings at spatial frequencies above (80 c/deg) and below (30 c/deg) the nominal Nyquist frequency for this array. No trace of aliasing was observed in the spectrum of the sampled 80 c/deg grating. The conclusion is that spatial disorder in foveal receptor placement allows alias-free sampling without introducing any appreciable spatial noise.

When a continuous optical image is reconstructed from values sampled at discrete points, mismatches between image bandwidth and sampling rate can give rise to a distortion known as "aliasing" whereby high spatial frequencies in the original image appear as low spatial frequencies in its reconstruction (Pearson, 1975; Yellott *et al.*, 1982). A familiar example is the Moiré distortion sometimes seen in television pictures of high frequency objects such as a tweed coat. Aliasing is caused by undersampling: it occurs when the sampling rate provided by a regular array of points is less than twice the highest spatial frequency imaged on that array. As a concrete example consider a square lattice of sample points spaced s units apart. The sampling theorem of information theory shows that such an array allows perfect reconstruction of any image whose highest spatial frequency is less than $(2s)^{-1}$ (Goodman, 1965). However if spatial frequencies higher than $(2s)^{-1}$ are imaged on this array the sample values recorded will be identical to those normally produced by specific lower frequencies (i.e. frequencies $<(2s)^{-1}$). Any reconstruction based on these sample values will necessarily confuse these sampling artifacts with genuine low frequencies. For example a vertical grating with frequency $f > (2s)^{-1}$ will yield exactly the same sample values as a grating with frequency $s^{-1} - f$ (see Fig. 1, Panels E and F) and no post-sampling process will be able to distinguish between a real $(s^{-1} - f)$ grating and one generated by aliasing. The aliasing cutoff frequency of a sampling array (i.e. $(2s)^{-1}$ in this example) is called its Nyquist frequency.

Because aliasing cannot readily be corrected by post-sampling operations it imposes fundamental constraints on the design of image transmission systems. The normal engineering solution is to ensure that spatial frequencies above the Nyquist frequency never reach the sampling array by bandlimiting the

image at the optical stage—i.e. frequencies that would otherwise be aliased are filtered out by the optical transfer function of the camera (Schade, 1975).

Vertebrate vision begins with the sampling of continuous retinal images by discrete arrays of photoreceptors. Consequently aliasing poses the same design problem here as in artificial image processing systems. However the parameters of the human eye indicate that our visual system does not solve its aliasing problem by the standard engineering technique of bandlimiting the optical image to match the Nyquist frequency of its sampling array. On the contrary, over much of the retina there is a large mismatch between the optically imposed bandwidth limits of the retinal image and the Nyquist frequencies implied by the total number of photoreceptors available to sample that image. Only in the center of the fovea (the foveola) is this not so: there the mean inter-receptor distance (center-to-center) is $(120)^{-1}$ deg of visual angle (Osterberg, 1935) and ophthalmoscopic measurements indicate that the foveal optical transfer function of the eye vanishes at 60 ± 10 c/deg (Campbell and Gubisch, 1966; Gubisch, 1967). In this tiny region then there is a good fit between the nominal Nyquist frequency of the receptor array and the bandwidth of the images that can be formed on that array in normal vision. Outside the foveola, however, cone density falls off precipitously while retinal image quality remains roughly constant for some 25 deg (Jennings and Charman, 1981). For example at 6 deg eccentricity the mean inter-cone distance has increased to $(30)^{-1}$ deg, implying a Nyquist frequency of 15 c/deg, whereas the optical transfer function cutoff is still 60 c/deg. Thus one would expect that if the cones formed a locally regular sampling array, extrafoveal photopic vision should be plagued by aliasing—e.g. at 6 deg eccentricity, 25 c/deg should alias back to 5 c/deg, and since that frequency is

detectible when it is actually present on the retina at this eccentricity (Green, 1970) it should also be detectible—and usually troublesome—when it is present as an artifact of aliasing. But nothing like this occurs in normal vision, and when extrafoveal acuity is measured experimentally there is no evidence that spatial frequencies above the local Nyquist limits can be detected in the guise of their sub-Nyquist aliases. Evidentally despite the mismatch between extrafoveal image bandwidth and receptor density the visual system somehow manages to prevent aliasing.

There is also evidence that even in the central fovea, the visual system does not actually rely on the bandlimits imposed by its optics to prevent aliasing. Using coherent light it is possible to bypass the optics of the eye and image spatial frequencies well above 60 c/deg directly on the retina in the form of interference patterns. When visual acuity is measured under these conditions the foveal limit remains 60 c/deg, just as in normal vision (Campbell and Green, 1965; Westheimer, 1960). If the receptors here formed a regular sampling array this would not be expected because higher frequencies should alias back into the detectible range—e.g. 90 c/deg should be detected as 30 c/deg, etc. Apparently even in the fovea aliasing is forestalled by post-optical factors.

How might the visual system prevent aliasing? Three factors must be considered: receptor size, receptor placement, and post-sampling neural mechanisms. Effects of receptor size can be calculated by assuming that each receptor integrates light over a disk-shaped region corresponding to its cross-sectional area. The result will be a reduction in effective grating contrast by a factor of $2J_1(\pi df)/(\pi df)$ where f is the spatial frequency of the grating, d is receptor diameter and J_1 is the first order Bessel function. In the foveola d averages $(240)^{-1}$ deg (Polyak, 1957), implying contrast reduction factors of 0.9 at $f = 60$ c/deg and 0.7 at $f = 120$ c/deg. Thus frequencies in the range 60–120 c/deg should be aliased back with very little reduction in contrast, e.g. a 110 c/deg 100% contrast interference grating should be indistinguishable from a 10 c/deg grating with a contrast of roughly 77%, which is readily detectible in normal vision. Outside the foveola cone diameters increase somewhat, but the net impact on potential aliasing is even more negligible: at 6°, for instance, $d \approx (120)^{-1}$ deg (Polyak, 1957), implying a contrast reduction factor of 0.97 at the local Nyquist frequency (15 c/deg) and 0.93 at 30 c/deg. From these calculations it seems clear that light integration over receptor surface areas cannot play any significant role in preventing the aliasing of spatial frequencies ranging for least an octave above the nominal Nyquist limits of the retina.

Photoreceptor spacing is a much more promising candidate: human receptors clearly do not form a perfectly regular sampling array (Fig. 1A) and random departures from spatial regularity can definitely eliminate aliasing—in effect by scattering potential aliased frequencies into broadband noise (Nagel,

1982). Conventional photography provides a familiar demonstration: there continuous optical images are sampled by randomly placed silver halide chrystals and the problem of aliasing does not arise; low mean sampling rates yield noisier images but no harmonic distortion. However it is not obvious *a priori* that actual photoreceptor arrays are sufficiently disorderly to guarantee alias-free sampling. Random placement *per se* is not enough for this purpose, as can be seen in panels E and F of Fig. 1, which illustrate the consequences of sampling gratings with a somewhat imperfect square array of points created by hand-poking pinholes in a sheet of black paper. Here each pinhole varies by a random amount from its ideal lattice position but aliasing is clearly apparent in Panel F. Suppression of aliasing by topological disorder requires randomness of a certain kind (Scott, 1976). Poisson distribution of the sample points (as in photographic film) is one example, but human receptor placement is far from Poisson and so it is an empirical question whether their actual spatial disorder is sufficient to prevent aliasing.

To provide evidence on this question I have calculated the power spectrum (square modulus of the Fourier transform) of an array of human foveal cones treated as sample points, and also the power spectra of gratings at spatial frequencies below and above the nominal Nyquist frequency for this array. i.e. the spectra of these gratings as they would appear after sampling by the photoreceptors. These power spectra were compared with those of the same pair of gratings as they would appear after sampling by a regular square array of points having the same spacing as the average value for the real receptor array. The procedure and results of this analysis are illustrated in Figs 1 and 2. Figure 1A shows a photomicrograph of a $12' \times 13'$ patch of foveal cones prepared by Polyak (1957, p. 268). This patch was located almost at the center of the foveala: mean center to center distance between cones is $0.56'$ [$(107)^{-1}$ deg], implying a nominal Nyquist frequency of 54 c/deg. Pinholes were punched through black paper at the apparent center of each receptor in this array. On the scale of the retina the pinhole diameters averaged roughly $0.2'$, as compared with an average cone diameter of $0.4'$. (Thus this simulated receptor array would be somewhat more likely to display aliasing than the cones on which it was based.) Figure 1B shows the resulting array of sample points. This pinhole array was then placed on top of 100% contrast square wave gratings having fundamental frequencies of 30 c/deg (on the scale of the retina) and 80 c/deg and the resulting "sandwiches" were photographed on a light table. (Strips at the top of panels C and D illustrate the gratings.) Figure 1C shows the results of sampling 30 c/deg with this array: the sampled grating is clearly a good rough facsimile of the original. Figure 1D shows the sampled version of 80 c/deg: here the periodic structure of the original grating has obviously been distorted by the sampling process. However it is
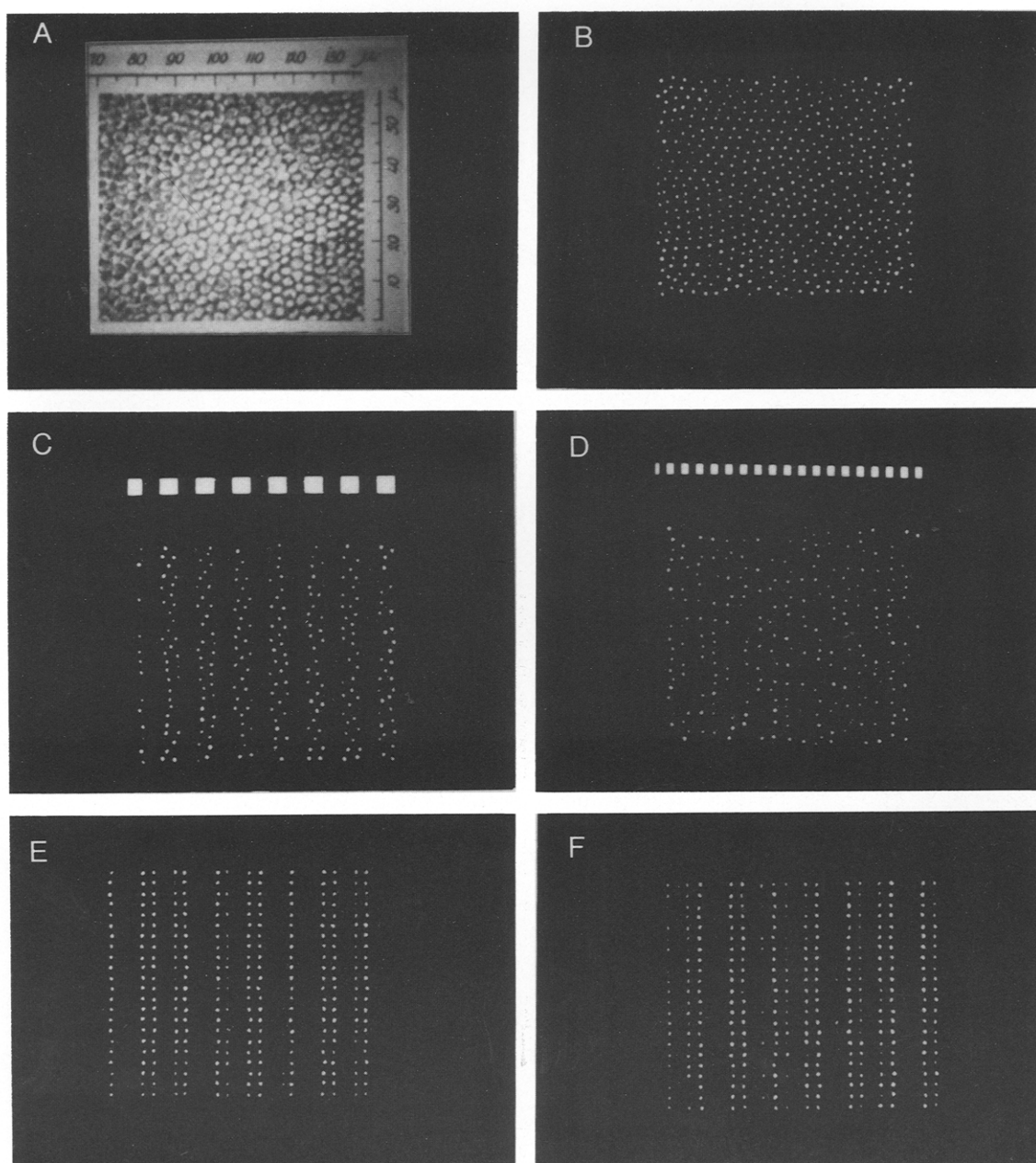
Fig. 1. (A) 12′ × 13′ patch of human foveal cones seen end-on. (Photomicrograph by Polyak, 1957, Fig. 156. (B) Array of sample points created by poking pinholes though the centers of the cones in Panel A. (C) 30 c/deg square wave grating seen through the pinhole sampling array of Panel B. Thin strip at top illustrates the spacing of the grating. (D) 80 c/deg square wave grating seen through the pinhole sampling array of Panel B. Strip at top illustrates the spacing of the grating. (E) 30 c/deg square wave grating seen through a regular square array of pinholes whose spacing matches the average value of the interpoint distances in Panel A. The grating is the same as in Panel C. (F) 80 c/deg square wave grating seen through the same regular square array used in Panel E. The grating is the same as in Panel D.
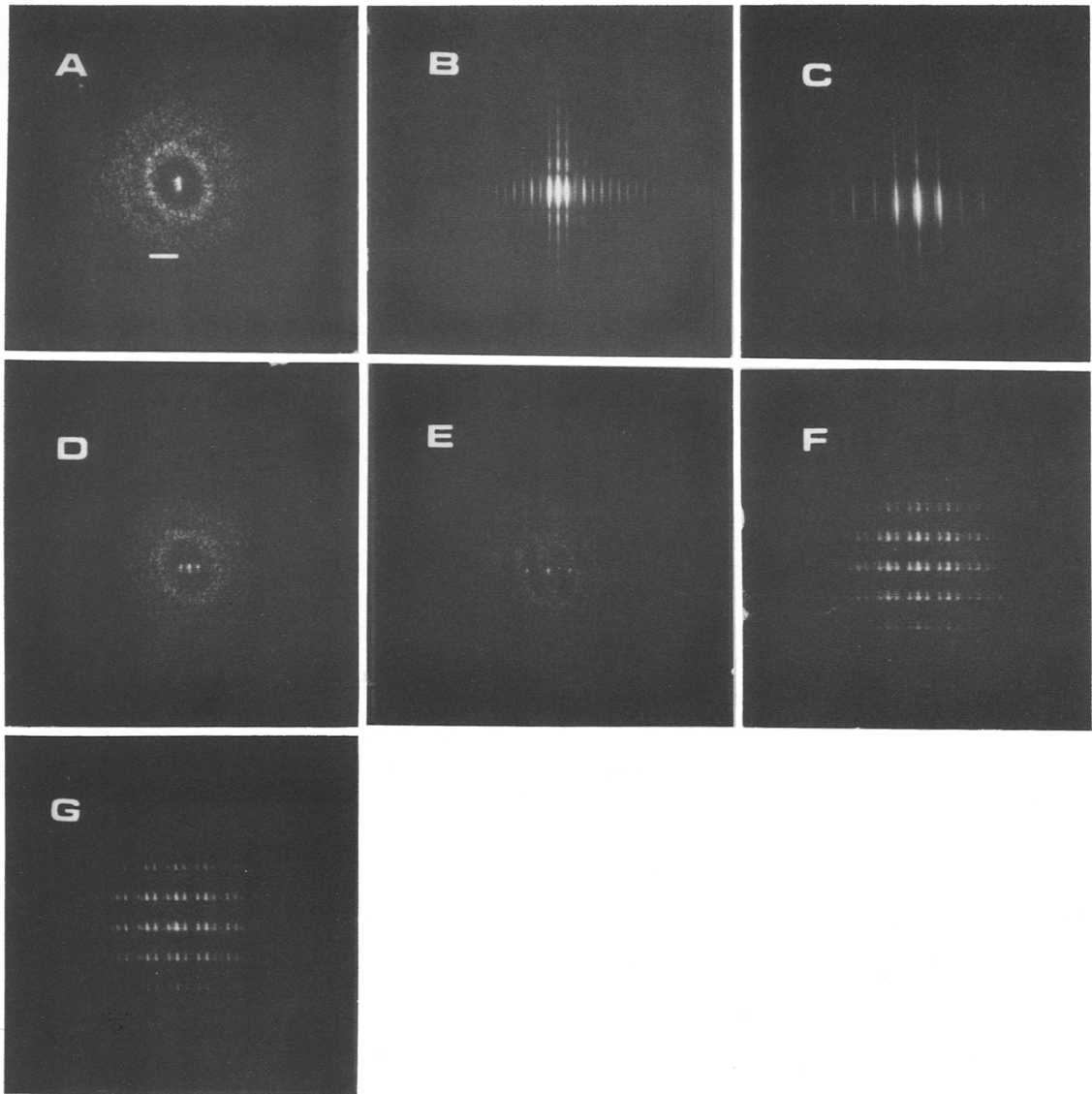
Fig. 2. (A) Power spectrum (optical transform) of the simulated receptor sampling array shown in Fig. 1B. Horizontal strip at bottom left indicates a distance of 100 c/deg. (B) Power spectrum of the thin strip of 30 c/deg square wave grating shown in Fig. 1C. (C) Power spectrum of the strip of 80 c/deg square wave grating shown in Fig. 1D. (D) Power spectrum of the lower portion of Fig. 1C, i.e. of the 30 c/deg grating after sampling by the pinhole array of Fig. 1B. (E) Power spectrum of the lower portion of Fig. 1D, i.e. of the 80 c/deg grating after sampling by the pinhole array of Fig. 1B. (F) Power spectrum of Fig. 1E, i.e. of the 30 c/deg grating after sampling by a regular square array of points. (G) Power spectrum of Fig. 1F, i.e. of the 80 c/deg grating after sampling by a regular square array of points.

1208

not obvious from inspection whether aliasing has taken place. Certainly panel D does not look like a 27 c/deg (i.e. $107 - 80 = d^{-1} - f$) vertical grating as it would in classical aliasing. (By comparison panels D and E illustrate the results of sampling 30 and 80 c/deg with an approximately regular square array of pinholes whose spacing is roughly 0.56' on the scale of the retina. Here aliasing is clear-cut: the sampled version of 80 c/deg is indistinguishable from the sampled version of 30 c/deg). On the other hand Panel D does not look like a uniform field or like 80 c/deg, and one cannot readily determine by eye whether any spectral energy has been aliased back to 27 c/deg.

To answer this question Panels B–F of Fig. 1 were photographically reduced to high contrast transparencies approximately 1 cm^2 and the power spectrum of each panel was computed in the form of an optical transform using standard techniques (Harburn et al., 1975). Coherent light from a 4 mW He–Ne laser (Spectra Physics model 248) was diverged, collimated, passed through each transparency, and the resulting diffraction pattern (optical transform) was imaged on the far side by a plus lens. An enlarged image of the optical transform was then cast on a distant rear projection screen and photographed with Polaroid P/N 55 film. Figure 2 shows the results. Panel A is the power spectrum of the receptor array itself (i.e. of Fig. 1B): it consists of a sharp spike at the origin surrounded by a roughly circular island of empty space having a radius of approximately 100–110 c/deg. Outside this island a broad annulus of uniform random noise begins abruptly and extends out to around 150 c/deg. This spectrum is particularly important because it can be used to calculate the effects of sampling any image with the corresponding array of photoreceptors: the power spectrum of a sampled image will be the convolution of the spectrum of the original image with the spectrum of the sampling array (Nagel, 1982; Scott, 1976). Panels B and C respectively show the power spectra of the narrow strips of 30 and 80 c/deg gratings contained in Panels C and D of Fig. 1. These spectra provided a scale for the other transforms: both show energy peaks (along the horizontal axis) at the origin, at the fundamental frequencies of the corresponding gratings (i.e. at ±30 c/deg in Panel B and at ±80 c/deg in Panel C), and at integer multiples of those frequencies. (Even harmonics do not vanish here because of slight width differences between the black and white bars of the gratings. Dilation of the spectra along the vertical axis is due to the fact that these are spectra of gratings seen through narrow horizontal windows.) Panel D shows the spectrum of the 30 c/deg grating sampled by the receptor array (i.e. the spectrum of Fig. 1C): isolated peaks appear at the origin and ±30 c/deg and there is no other concentration of signal power. Panel E is the object of greatest interest: it shows the spectrum of 80 c/deg after sampling by the receptor array (i.e. Panel D in Fig. 1). If aliasing were occurring power concentrations would be expected at

±27 c/deg. In fact there is no sign of this; the only sharp concentrations of spectral energy fall at ±80 c/deg (and at the origin) and it is evident that the potential aliased energy at ±27 c/deg has been scattered into broad band noise. By contrast, Panels F and G show the spectra of the 30 and 80 c/deg gratings after sampling by a regular square array (i.e. the spectra of Figs 1E and 1F respectively). These two spectra are essentially indistinguishable, reflecting the strong aliasing of 80 c/deg back to 27 c/deg that would be expected with this sampling array.

Evidentally the array of cones analyzed here (an array Polyak regarded as typical of the human foveola) is sufficiently disorderly to prevent aliasing. In addition Fig. 2E indicates that the foveal cones, considered as an array of sample points, are capable of transmitting spatial frequencies well above their nominal Nyquist frequency of 60 c/deg. Consequently the 60 c/deg visual acuity limit obtained with interference fringe targets is most likely due to neural filtering mechanisms operating beyond the quantum catch stage. This conclusion agrees with the results of Ohzu and Enoch (Ohzu and Enoch, 1972), who calculated modulation transfer functions of freshly excised human foveas using a different but logically parallel technique. Finally the parameters of the power spectrum of the foveal array shown in Fig. 2A suggest that the visual system has evolved an optimally random distribution of photoreceptors: the configuration of this spectrum implies that sampling by foveal receptors will introduce virtually no sampling noise for spatial frequencies below 50–60 c/deg, i.e. for the frequencies present in normal retinal images. It remains to be seen whether extrafoveal receptor arrays also exhibit the same alias-free, noise-free sampling characteristics.

REFERENCES

Campbell F. W. and Green D. G. (1965) Optical and retinal factors affecting visual resolution. J. Physiol., Lond. 181, 576–593.

Campbell F. W. and Gubisch R. W. (1966) Optical quality of the human eye. J. Physiol., Lond. 197, 558–578.

Goodman J. W. (1965) Introduction to Fourier Optics. McGraw-Hill, New York.

Green D. G. (1970) Regional variations in the visual acuity for interference fringes on the retina. J. Physiol., Lond. 207, 351–356.

Gubisch R. W. (1967) Optical performance of the human eye. J. opt. Soc. Am. 57, 407–415.

Harburn G., Taylor C. A. and Welberry T. R. (1975) Atlas of Optical Transforms. Cornell Univ. Press, Ithaca, NY.

Jennings J. A. M. and Charman W. N. (1981) Off-axis image quality in the human eye. Vision Res. 21, 445–455.

Nagel D. (1982) Spatial sampling in the retina. J. opt. Soc. Am. In press.

Ohzu H. and Enoch J. M. (1972) Optical modulation by the isolated human fovea. *Vision Res.* **12,** 245–251.

Osterberg G. (1935) Topography of the layer of rods and cones in the human retina. *Acta ophthal., Suppl.* **6,** 11–97.

Pearson D. E. (1975) *Transmission and Display of Pictorial Information.* Wiley, New York.

Polyak S. L. (1957) *The Vertebrate Visual System.* Univ. of Chicago Press, Chicago.

Schade O. H. (1975) *Image Quality: A Comparison of Photographic and Television Systems.* RCA Laboratories, Princeton, NJ.

Scott P. F. (1976) *Distribution and Estimation of the Autocorrelation Function of a Randomly Sampled Signal.* Report No. 76CRD180, General Electric Co., Schenectady, NY.

Westheimer G. (1960) Modulation thresholds for sinusoidal light distribution on the retina. *J. Physiol., Lond.* **152,** 67–74.

Yellott J. I., Wandell B. and Cornsweet T. (1982) The beginnings of visual perception: the retinal image and its initial encoding. In *Handbook of Physiology—The Nervous System* III American Physiological Society. In press.